Surface functionalization of handleable silica-based mesoporous materials for CO2 sequestration: Synthesis, characterization and performance

Surface functionalization of handleable silica-based mesoporous materials for CO_2 sequestration: synthesis, characterization and performance.

Razieh Sadraei[1,2], Fabio Cucchiara[1], Giuliana Magnacca[1], Maria Luisa Testa[3]

[1] Dipartimento di Chimica and NIS Interdepartmental Centre, Università di Torino, via P. Giuria 7, 10125 Torino, Italy; fcucchiara561@gmail.com (F.C.), giuliana.magnacca@unito.it (G.M.)

[2] Current address: Faculty of Science, Engineering and computing, Kingston University, River House,53-57 High Street, Kingston upon Thames, Surrey KT1 1LQ, United Kingdom; r.sadraei@kingston.ac.uk (R.S.)

[3] Istituto per lo Studio dei Materiali Nanostrutturati, Consiglio Nazionale delle Ricerche, via U. La Malfa 153, 90146 Palermo, Italy; marialuisa.testa@cnr.it (M.L.T.)

Abstract:

Two different types of silica monolith based on commercial hydrophobic Aerosil200 and hydrophilic Sipernat320 (Evonik) were successfully covalently functionalized with different amines as CO_2 sequestrants. 3-aminopropyltriethoxysilane (AMPS) was used for a first functionalization and applied as it is or as linker to extend the chain length with diglycine (diGly) and triglycine (triGly). The physico-chemical characterization of the samples comprehends nitrogen adsorption at -196°C to determine surface area and porosity and thermogravimetric analysis (TGA) to evaluate the thermal stability of the materials and quantify the extent of functionalization. CO_2 and N_2 adsorption microcalorimetry, coupled with FTIR spectroscopy, was used to evaluate the ability of the materials to selectively sequestrate CO_2 against N_2 in post-combustion procedures and the reversibility of the process. The comparison with a powdery commercial activated carbon, taken as reference, evidences the good adsorption capacity (comparable to that of the carbon reference) of monoliths from Sipernat 320 bringing a short aliphatic chain and terminal $-NH_2$ groups (more than 700 μmol/g of CO_2 sequestrated at 30°C), and the advantages in term of easy storage and recoverability, with respect to powdery adsorbents.

Keywords: Silica monolith, surface functionalization, Aerosil200, Sipernat320, CO_2 adsorption, amine immobilization.

1. *Introduction*

The greenhouse gases such as CO_2, CH_4, N_2O, sulfur hexafluorides and chlorofluorocarbons have been considered as the main important cause of climate alteration crisis influenced by global warming. The 80% of CO_2 present in the atmosphere is produced in still widely used industrial processes and burning of fossil fuels [1-3], it remains in the atmosphere for remarkable longer period with respect to other greenhouse gases, and therefore CO_2 plays, among the others, the major detrimental role [4].

To limit these effects, CO_2 needs to be produced in lower amounts, but until when sources of energy alternative to fossil fuels are not properly developed and widely diffused, it needs to be captured. The state of the art on the sequestration of CO_2 includes the use of aqueous amine solutions which are able to chemically absorb CO_2 [5]. Although this technique is the most mature CO_2 sequestration technology, it shows serious drawbacks including a high energy consumption needed for desorption, as well as corrosion of process equipment [6]. An alternative technology is given by ionic liquids, salts in liquid phase, whose composition can be modulated to enhance the affinity, and consequently the capture efficiency, towards CO_2 [7]. This technology is still under study, but promises enhanced performance. Another evergreen, effective approach is based on adsorption on solid materials, as, in general, it allows to overcome several issues maintaining limited costs. Adsorption technology based on porous adsorbents seems to be very advantageous [8-9], however, the efficiency of this method depends on development of novel adsorbent materials feasible to be potentially used at a large scale in industrial plants. Many porous adsorbents, such as Metal-Organic Frameworks [10], carbon materials [11], amine-functionalized zeolites [12], activated carbons [13-15], alkali-metal-based solid sorbents [16], carbonate slurry [17], N-doped activated carbon [6], polymer or aminopolymer/silica composite [18], alkali earth metal oxides [19], sulfur-doped activated carbon [20] and microporous covalent polymer [21], have been reported for CO_2 capture. Although activated carbons are proven to possess tunable features due to high surface area, chemical stability and presence of chemical groups enhancing the affinity towards CO_2, a high energy cost and non-ecofriendly treatments are required for their preparation [2]. In addition, activated carbon in powdery form can generate a remarkable pressure drop in the gas stream used in columns [5, 22], therefore a further step of material shaping needs to be taken into consideration in the production procedure. In order to overcome these drawbacks, development of other adsorbents, environmentally friendly, more handleable, cost effective, low energy consuming and easy to produce in large quantity, appears very attractive [2]. In this respect, functionalized silica monolith materials emerged as promising porous adsorbent for CO_2 capture. Silica supports have several advantaged over other inorganic materials: they possess high surface area, can be

meso or macroporous, are structurally stable in a large range of temperatures as sintering, and the consequent lack of surface area and porosity, occurs only at temperatures higher than 800°C. Moreover, silica surface carries silanol groups which can be easily chemically modified by functionalization procedures [23]. Depending on the introduced functionalizing groups, it is possible to completely transform the starting physical and/or chemical properties of the original system [24-27].

Recently, organic moieties like alkyl, phenyl, vinyl, methacrylate, amine, sulfone, thiol and metal-ligand complexes have been employed to functionalize porous silicas. Among all, amines are the most suitable to deal with CO_2 removal [28-31], but in a wider view, amines are highly active in the removal of metals from environmental waste [32-33], removal of organic dyes [34], they can be used in chromatography [35], gas separation, catalysis [36], drug release [37-38], and many other applications [39-40], therefore the study of the functionalization of a support with amine groups can be of general interest for the scientific community.

The preparation of amine-functionalized silica (AFS) can be realized through various methods divided into two main groups: i) physical procedures, which imply the establishment of simple electrostatic interactions between the support surface and the functionalizing molecules [41-43] and ii) chemical functionalization, which leads to the formation of stable covalent bonds between the support and the organic groups. In detail, it can proceed through two main chemical strategies: co-condensation technique [44-45] or post-synthesis functionalization (grafting) [46-48]. Through the first method, the material is functionalized at the same time of its formation and this implies that the functionalizing groups are homogeneously dispersed in the whole system. On the contrary, when the grafting procedure is used, the functional groups are located only at the surface of the material.

Testa et al. described the preparation of AFS using different kinds of silica powders including amorphous silica, HMS and SBA-15 (both mesoporous with ordered porosity) as intermediate for the immobilization of photoactive molecules applied in the abatement of 4-methylphenol [49], rhodamine and metals [50]. Testa again studied the different grafting and in situ oxidation procedures [51]. In another study SBA-15 was functionalized by post-grafting method with three different alkoxysilanes, including (3-aminopropyl)triethoxysilane, 3-[bis(2-hydroxyethyl)amino] propyl triethoxysilane and 3-[2-(2-aminoethylamino] propyl trimethoxysilane for drug delivery application [52].

Different types of silica can react differently towards the functionalization, consequently affecting the final material performance. Although powdery silica is still under use as a support for surface functionalization processes [53-54], it shows severe drawbacks, including the difficulty of recovery the powdery materials after adsorption process which implies increasing process costs and time wasting. Therefore, researchers are developing several processes to prepare handleable systems for substituting silica powders [55-58]. In this perspective, Magnacca et al. developed an interesting method

to prepare silica monoliths by using Bio-Based Substances (BBS), extracted from composted biowastes, as binders [59]. In that study, BBS act as biosurfactant and templating agent, forming micelles around which the preformed silica particles can agglomerate, and as fusion salt supplier. During the calcination step, the fusion salts of the BBS allow the partial fusion of the silica particles whereas the organic moieties burn leaving void space. By using this procedure, handleable and mesoporous silica supports are produced and constitute a versatile platform to be used in a wide range of applications. The materials were prepared starting from two commercial silicas, the more hydrophobic Aerosil 200 and the more hydrophilic Sipernat 320 (both from Evonik). Due to the impurities derived from BBS inorganic components (Na^+, K^+, Ca^{2+}, Mg^{2+}), the materials contain cationic species which can increase the basicity of the surface creating a favorable situation for CO_2 uptake, but also a possible interference to the surface functionalization process. For this reason, the chemical functionalization of the monoliths was carried out following grafting procedures already tested and reported in the literature, in order to evaluate their efficacy. In particular, 3-aminopropyltriethoxysilane (AMPS) was used for a first functionalization and applied as a direct functionalizing agent or as linker to extend the chain length with diglycine (diGly) and triglycine (triGly). After functionalization, the hybrid monoliths were characterized in terms of textural properties and loading of the organic portion and then tested towards CO_2 and N_2 adsorption at 30°C. The results were compared with those obtained with the non-functionalised monoliths.

2. Experimental

2.1. Materials

Two different commercially available silica samples were used for monolith preparation: Aerosil200 (A200) with BET surface area (SSA) of 200 m^2/g and FK320 (actual commercial name Sipernat320) with SSA of 160 m^2/g. Both powders were kindly supplied by Evonik. Amine derivatives (AMPS, Diglycine and Triglycine), N-ethyl-N'-(3-dimethylaminopropyl)carbodiimide chloride (EDC) and solvents were purchased from Sigma-Aldrich (Milan, Italy). Solvents (toluene and ethanol) were distilled prior the use.

2.2. Preparation of monoliths

The monolith preparation procedure has been already reported in the literature [59] and it will be briefly reported here.

2 g of BBS were stirred in 30 ml of water for 2 hours. 8 g of silica particles (A200/FK320) were added to the BBS solution. 50 ml of water were then added and the mixture was kept under stirring for 2 h. The systems exhibited thixotropic behavior with high viscosity and vigorous stirring was needed to achieve an efficient mixing of the

suspensions. The mixture was then left during one night, until the suspension dried sufficiently to be easily modeled: brown spheres of 5 mm diameter were hand-molded, left at air for drying and then calcined in a furnace at 500°C for 4 hours in order to remove all organic moieties and yield porous monoliths designated as A and FK. The spheres after calcination appear pale grey in color. A detail of the monolith surface appears in Figure 1: FK monoliths are more regular and homogeneous with respect to A ones, reflecting a better mechanical stability of the system.

The experiment was carried out in duplicate, in order to evaluate the reproducibility of the preparation method which was proven after the characterization.

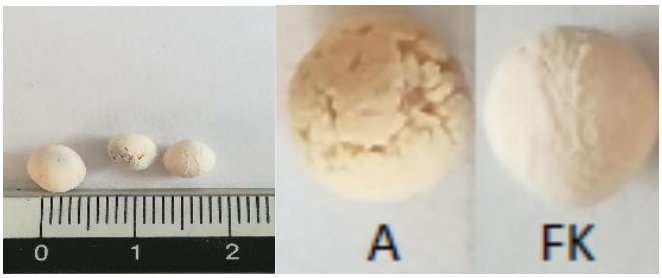

Figure 1. Monoliths (left image) and details of A and FK surface (right image).

2.3. Monolith functionalization process

2.3.1. Functionalization by AMPS

A and FK were functionalized with AMPS through adopting the optimized grafting method reported in the literature [49]. In a typical procedure, a mixture of 3.2 g of monoliths in 20 ml of dry toluene and 6.3 ml of AMPS ($2.7*10^{-2}$ mol) was refluxed overnight at 110°C under low speed stirring in order to prevent monolith breaking. The samples were separated from the mixture of reaction, washed with ethanol and dried at 110°C overnight. The obtained samples are indicated as A-NH_2 and FK-NH_2.

2.3.2. Chain extension on samples A-NH_2 and FK-NH_2 with diGly and triGly

The extension of the organic chain was carried out for samples A-NH_2 and FK-NH_2 by using diGlycine and triGlycine. 0.37 g ($2*10^{-3}$ mol) of diGly or triGly, respectively, and 0.09 g ($4*10^{-4}$ mol) of N-ethyl-N'-(3-dimethylaminopropyl)carbodiimide chloride (EDC) were added to a suspension of 1.0 g of amino functionalized monoliths in 50 mL of toluene. The mixture was refluxed for 12 h. The material was separated from the mixture and washed several times with toluene, ethanol and sodium chloride solution (1 M), then dried in oven at 100 °C overnight. The samples are named A-$(Gly)_x$-NH_2 and FK-$(Gly)_x$-NH_2, with x=2 or 3 respectively.

Scheme 1 reports the summary of the functionalized procedures, whereas Table 1 reports the name of the samples, the functionalizing agents used and the functional groups introduced on the surface of the monoliths.

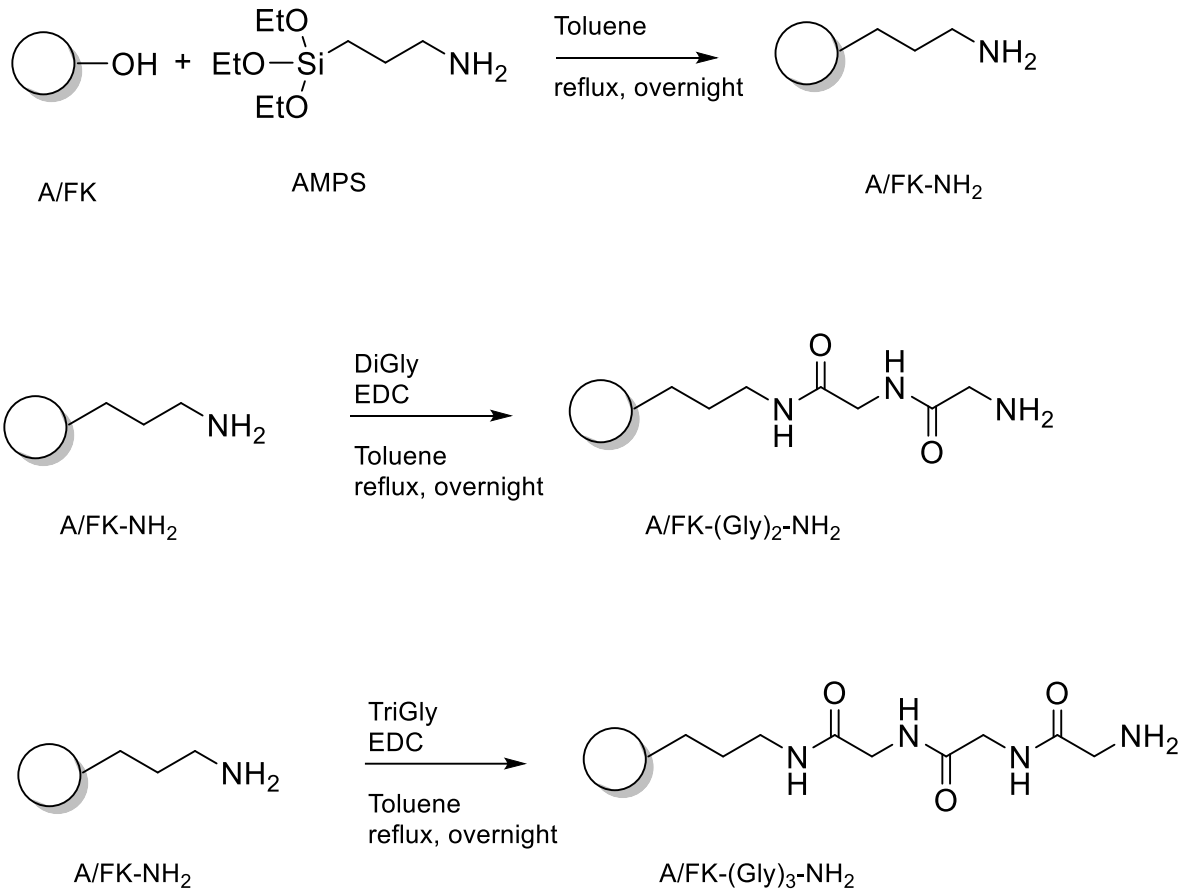

Scheme 1. Schematic representation of functionalization processes.

Table 1. Sample names, functionalizing agent and functional groups introduced on the surface of the monoliths

Sample name	***Functionalizing agent/support***	***Exposed functional groups***
A	-	-
FK		-
A-NH2	AMPS/A	-NH_2
FK-NH2	AMPS/FK	-NH_2

A-(Gly)$_2$-NH$_2$	Gly-Gly/A	-NH-(Gly)$_2$-NH$_2$
FK-(Gly)$_2$-NH$_2$	Gly-Gly/FK	-NH-(Gly)$_2$-NH$_2$
A-(Gly)$_3$-NH$_2$	Gly-Gly-Gly/A	-NH-(Gly)$_3$-NH$_2$
FK-(Gly)$_3$-NH$_2$	Gly-Gly-Gly/FK	-NH-(Gly)$_3$-NH$_2$

2.4. Physico-chemical characterization

Nitrogen adsorption-desorption adsorption at -196°C was performed by means of Micromeritics ASAP 2020 gas-volumetric apparatus. Prior to the experiments, all the samples were activated at 100°C for 3 h in order to eliminate gaseous contaminants adsorbed at the sample surface or filling the pores. Specific surface areas (SSA) were calculated by applying the Brunauer, Emmett, and Teller (BET) model, Total Pore Volume and Pore Size Distribution were determined by using the Barrett, Joyner, and Halenda model applied to the isotherm adsorption branch (Thommes et al., 2015).

Thermo-gravimetric analysis (TGA) was carried out by means of TA Q600 (TA Instruments) in the range 40-650°C with a heating rate of 10 °C/min under air.

2.5. Adsorption performance

CO_2 and N_2 adsorption gas-volumetric and calorimetric isotherms were determined using an adsorption microcalorimeter Tian-Calvet (Setaram, made in France) equipped with a lab-made gas-volumetric apparatus for evaluation of the adsorption isotherms [60]. More information about this method is given elsewhere [61].

3. Results and discussion

3.1. Physico-chemical characterization

3.1.1 Gas-volumetric adsorption of N_2 at -196°C

The isotherms obtained for A sample before and after functionalization with AMPS (as representative of all the functionalized samples) are reported in Figure 2 (left section) and present a shape of the IV type in the IUPAC classification, with hysteresis loop in the range of relative pressure p/p° = 0.75 – 1, indicative of the presence of mesopores.

The elaboration of the isotherms, via BET (for determining the specific surface area SSA of the samples) and BJH (for studying the total porosity and pore size distribution) models, gave the results reported in Table 2 and Figure 2 (right section). The SSA of A monolith after functionalization decreases of about 28%, with no significant and specific

effect due to the functionalizing molecule used. Analogously the total pore volume of the monoliths decreases after functionalization and the pore size distribution curves indicate that in all cases the functionalization causes the decrease of all the mesopores with disappearance of the smaller ones. The effect is evident after AMPS functionalization whereas the addition of Gly chain gives negligible effect not affecting significantly the SSA and porosity values with respect to A-NH_2 sample.

Table 2 reports all the calculated BET SSA and BJH total pore volume values.

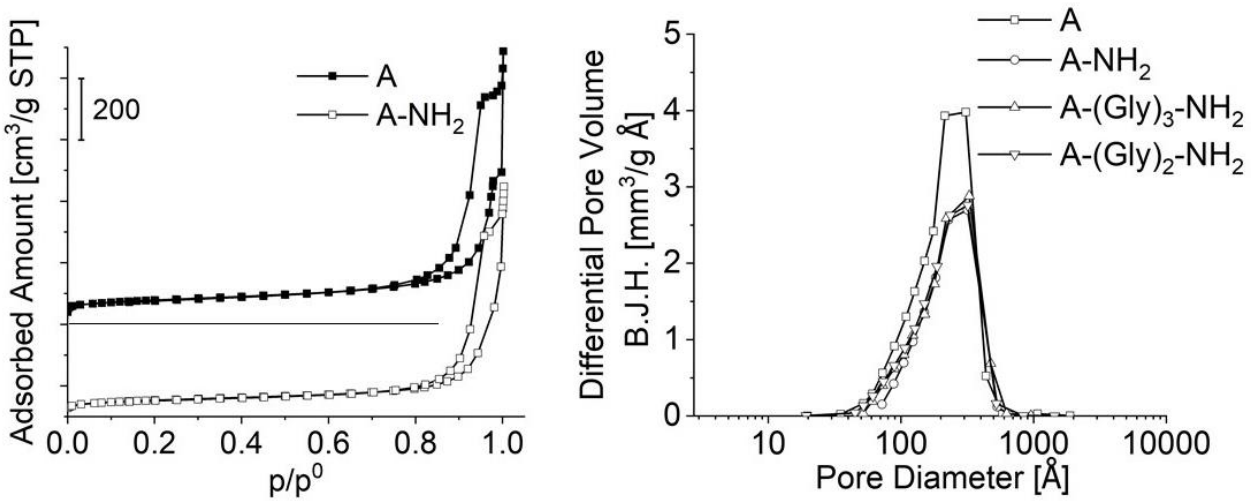

Figure 2: Left section: Adsorption isotherms for A and A-NH_2 samples. The curves are shifted for the sake of clarity: the horizontal line was inserted as a reference of the origin of the y-axis relatively to A isotherm. Right section: Pore size distribution curves for A before and after functionalization.

Also in the case of FK-based materials, the adsorption isotherms of the FK monolith before and after functionalization with AMPS (as representative of the functionalized samples), compared in Figure 3 (left section), are of the IV type in the IUPAC classification indicating the presence of mesopores. The hysteresis loop present at high p/p° value changes significantly after functionalization giving the pore size distribution curves reported in Figure 3 (right section). Contrary to the previous case, the functionalization with AMPS and AMPS-triGly causes the appearance of a larger porosity with respect to the unmodified monolith, probably because the functionalizing molecules are able in creating a network revealed by N_2 as macropores. Otherwise, the other functionalizing agents cause the expected effect already described above, with the decrease of the amount of mesopores and the disappearance of the smaller pores. The values of SSA and BJH total pore volume are reported in Table 2 indicating also the decrease of the SSA and porosity after functionalization. The effect is particularly evident after AMPS functionalization.

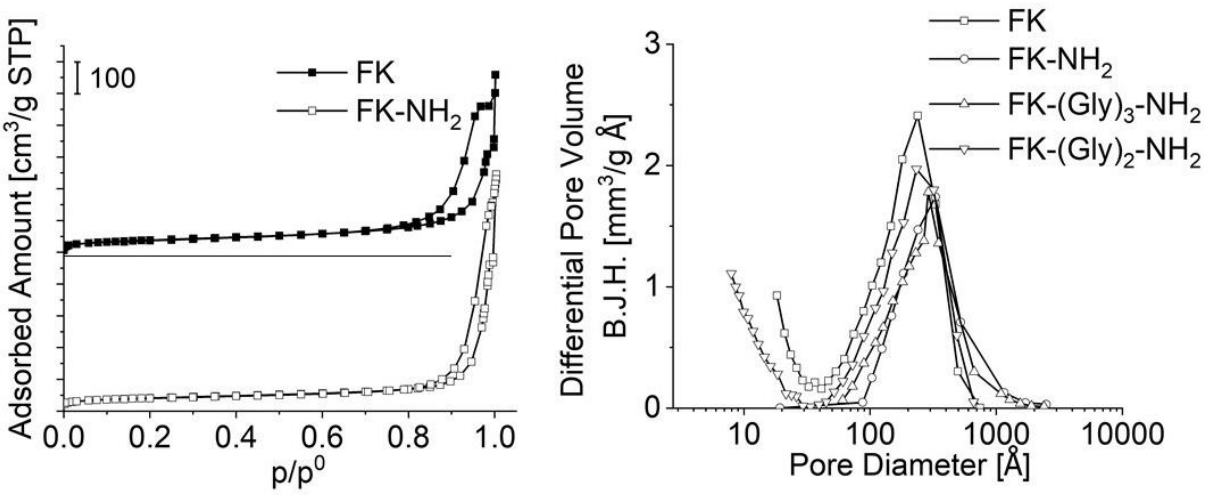

Figure 3: Left section: Adsorption isotherms for A and A-NH_2 samples. The curves are shifted for the sake of clarity: the horizontal line was inserted as a reference of the origin of the y-axis relatively to FK isotherm. Right section: Pore size distribution curves for A before and after functionalization.

Table 2: Main results of the morphological characterization of monoliths before and after functionalization: BET SSA and BJH total pore volume values.

Sample	***BET SSA (m^2/g)***	***BJH total pore volume (cm^3/g)***
A	160	1.15
A-NH_2	111	0.98
A-$(Gly)_2$-NH_2	117	0.91
A-$(Gly)_3$-NH_2	113	0.89
FK	136	0.71
FK-NH_2	88	0.97
FK-$(Gly)_2$-NH_2	97	0.41
FK-$(Gly)_3$-NH_2	91	0.91

3.1.2. Thermogravimetric (TGA) analysis

TGA analysis provided to establish the loadings of the samples as well as their stability. A and FK monoliths were processed as bare or functionalized with amine derivatives. For the sake of comparison, the weight loss experienced by the non-functionalized monoliths is reported in Figure 4.

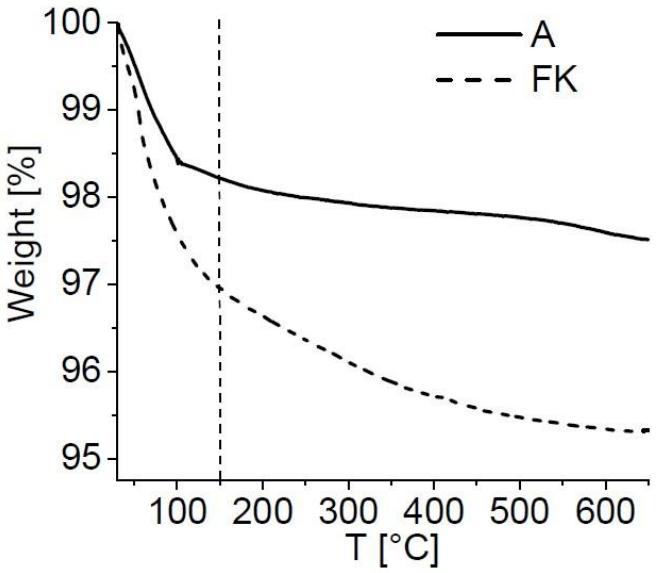

Figure 4: Residual weight of A and FK monoliths in the temperature range 30-650°C. The vertical broken line represents the value of 150°C, chosen as threshold to evaluate the amount of physisorbed water molecule eliminated by evaporation and the amount of OH groups eliminated by condensation.

Both of them show two important regions of weight loss, the first one in the range of 30-150°C, due to the removal of adsorbed water molecules from the surface of the materials, and the second one in the range of 150-650°C, due to elimination of OH group present at the surface of monoliths via condensation reaction. The nature of the two sillicas used for the preparation of the monoliths is different, as Aerosil is obtained by pyrolysis at high temperature whereas FK320 is produced by precipitation in aqueous media, therefore the first one is more hydrophobic whereas the second one is more hydrophilic. The different preparation methods reflect the obtained results: as expected, the amount of physisorbed water removed from A monolith (about 1.8%) is smaller than that removed from FK support (3.1%).

By employing Equation 1, we calculated the concentration of surface silanol groups (SiOH nm^{-2}) for non-functionalized monoliths:

$$\text{SiOH nm}^{-2} = \frac{\%OH}{100-\%OH} * \frac{2*N_A}{PM_{H2O}*SSA} \qquad \text{(Equation 1)}$$

where %OH represents the loss of H_2O due to the condensation of surface silanol groups (SiOH), 2 considers the number of silanol groups needed to form one water molecule, N_A is the Avogadro number ($6.022*10^{23}$ molecules mol^{-1}), PM_{H2O} is the molecular weight of water (18.01 g mol^{-1}) and SSA is the BET specific surface area expressed in nm^2 g^{-1}, determined by gas-volumetric N_2 measurement. The

concentration of surface silanol groups for the A monolith was 3.4 SiOH nm^{-2}, for FK monolith was 8.5 SiOH nm^{-2}. These values indicate the maximum capacity of monoliths in binding functionalizing molecules, as OH groups are the reactive sites for the covalent functionalization.

We applied the same procedure to functionalized monoliths in order to evaluate the amount of organic matter immobilized looking at the weight loss in the range 150-650°C. Figure 5 reports as an example the comparison between A200 before and after AMPS functionalization, as representative of all functionalized samples. The elaborations of the data are reported in Table 3.

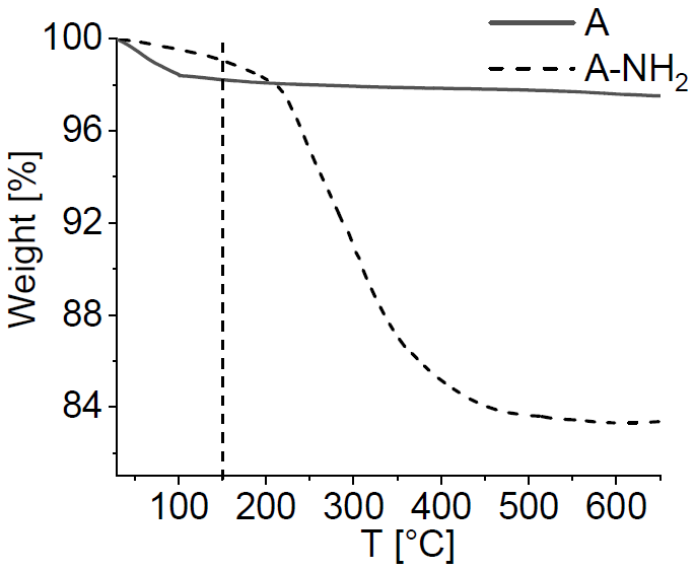

Figure 5: Residual weight of A monolith before and after functionalization with AMPS in the temperature range 30-650°C. The vertical black line represents the value of 150°C chosen as threshold to evaluate the amount of physisorbed water molecule eliminated by evaporation, the amount of OH groups eliminated by condensation (for non-functionalized support) and organics eliminated by decomposition (for functionalized materials).

Table 3: Percentage of weight loss and amounts expressed in groups nm^{-2} observed in terms of water molecule evaporation, OH groups condensation and organic matter decomposition.

Samples	***Physisorbed water amount (30-150°C) (% weight)***	***OH amount (150-650°C) (% weight)***	***Organic amount (150-650°C) (% weight)***	***OH amount (150-650°C) (groups g^{-1})***	***Organic amount (150-650°C) (groups g^{-1})***	***Chain extension (150-650°C) (groups g^{-1})***
A	1.8	0.8	-	$5.4\ 10^{20}$	-	-

A-NH$_2$	0.8	-	5.9	-	6.5 10^{20}	-
A-(Gly)$_2$-NH$_2$	0.8	-	9.1	-	4.3 10^{20}	5.54 10^{20}
A-(Gly)$_3$-NH$_2$	1.0	-	10.2	-	3.0 10^{20}	1.57 10^{20}
FK	3.1	1.7	-	11.6 10^{20}	-	-
FK-NH$_2$	2.6	-	8.2	-	9.3 10^{20}	-
FK-(Gly)$_2$-NH$_2$	0.9	-	9.3	-	4.4 10^{20}	0.58 10^{20}
FK-(Gly)$_3$-NH$_2$	0.9	-	9.1	-	2.6 10^{20}	0.32 10^{20}

The data corresponding to the loss of organic amount, reported in the sixth column of Table 4, are obtained considering Equation 2 and the following remarks: i) the OH groups of the supports are completely engaged in functionalization therefore no residual OH groups are present after functionalization reaction; ii) the functionalization extents is here reported for gram of sample; iii) the number of organic molecules introduced in the samples are calculated considering the weight of the fragment introduced on the surface. This means that the weight of the fragment -CH_2-CH_2-CH_2-NH_2 for –NH_2 samples is 58 g/mol, the weight of the fragment -CH_2-CH_2-CH_2-NH-CO-CH_2-NH-CO-CH_2-NH_2 for -$(Gly)_2$-NH_2 samples is 140 g/mol and the weight of the fragment -CH_2-CH_2-CH_2-NH-CO-CH_2-NH-CO-CH_2-NH-CO-CH_2-NH_2 for -$(Gly)_3$-NH_2 samples is 229 g/mol.

$$\text{Organic groups g}^{-1} = \frac{\%org}{100-\%org} * \frac{N_A}{PM_{fragment}} \qquad \text{(Equation 2)}$$

Results indicate that the functionalization yield of A support with AMPS was 100%, as we reached, apart the errors derived from the assumptions made, the maximum amount of support functionalization modifying all the OH groups present on the starting monolith. The functionalization yield in the case of the more hydrophilic FK support reached the 80%, lower, as expected considering the lower affinity of FK support with the apolar solvent used in the reaction (toluene).

The subsequent chain extension reactions carried out with diGly and triGly reached efficiencies definitely lower. Although the excess of reactants used for the functionalization process with respect to the number of reactive sites available for the process, we have to expect few long chains and several propylamino-groups unreacted

on the sample surface. In order to evaluate the efficiency of this chain extension reaction, we consider the weight loss of $–(Gly)_n-NH_2$ samples after subtraction of the weight loss observed for $–NH_2$ samples in the same 150-650°C temperature range. As described above, we consider the number of diGly and triGly reacted considering the weight of the extending fragments (namely $CO-CH_2-NH-CO-CH_2-NH_2$ for di(Gly) reaction, fragment weight of 115 g/mol, and $CO-CH_2-NH-CO-CH_2-NH-CO-CH_2-NH_2$ for triGly reaction, fragment weight of 172 g/mol). The values obtained from Equation 2 corresponding to the chain extension, are reported in the seventh column of Table 4. The efficiency of the reaction increases in the order triGly < diGly, so the number of residual short propylamino-chains is higher in the $–(Gly)_3-NH_2$ samples with respect to $–(Gly)_2-NH_2$ samples. More in detail, 85% of propylamino-groups underwent chain extension for A-$(Gly)_2-NH_2$ sample, 24% for A-$(Gly)_3-NH_2$ sample, 6% for FK-$(Gly)_2-NH_2$ sample and 3% for FK-$(Gly)_3-NH_2$ sample.

3.2. Adsorption of CO_2 and N_2 at 30°C

CO_2 adsorption capacity and related energy of CO_2-material interaction are measured using a Tian-Calvet microcalorimeter at the constant temperature of 30°C. These measurements were performed on the monoliths before and after functionalization in two runs: the first one (primary adsorption) immediately after the vacuum activation of the samples at 30°C, the second one (secondary adsorption) after the first run and a vacuum outgassing at the same temperature overnight. The vacuum outgassing should remove only CO_2 fraction reversibly (i.e., weakly) bonded to the material surface, whereas the irreversible fraction (i.e., the most strongly interacting with the surface) should remain attached leaving less sites available for secondary adsorption. Therefore, the difference between the two curves allows to evaluate the reversibility of the interaction as it corresponds to the amount of CO_2 irreversibly adsorbed by the sample at 30°C.

For evaluating the selectivity of the adsorption, also N_2 measurements were carried out: negligible adsorption was observed for all the samples confirming that amino-functionalized samples give specific interactions with CO_2 molecules and can, therefore, be applied for CO_2 removal from combustion downstream lines.

As an example, Figure 6 reports the main results obtained with gas-volumetric/microcalorimetric analyses. Figure 6, upper section, reports the adsorbed amounts as a function of equilibrium pressures, Figure 6, lower section, shows the interaction energies as a function of CO_2 coverage for the primary and secondary adsorption runs obtained for FK monoliths before and after AMPS functionalization. For simplifying the reading of the graphs, curves interpolating the experimental points were drawn down. As a result, the number of CO_2 molecules adsorbed on the functionalized monoliths is significantly higher than the number of CO_2 molecules adsorbed on the non-functionalized monoliths, but about 10% of the molecules interacts irreversibly with

the material at 30°C. The curves related to the heats of interaction CO_2-surface indicate a quite high energy evolved at low CO_2 coverage (the q° value extrapolated at zero coverage is about 130 kJ/mol), probably due to the formation of irreversibly bonded species, whereas an energy of less than 20 kJ/mol was evolved at higher CO_2 coverage, most likely due to the formation of reversibly bonded species. Actually, CO_2 can establish two types of interactions with oxide surfaces: via donation of oxygen lone pair to surface Lewis acid sites, namely cationic atoms of the surface (linear coordination), or via interaction of the carbon atom with surface basic sites, namely oxygen atoms of the surface (bent coordination). The activation of the sample at 30°C is not enough to make available strong Lewis acid sites for CO_2 interactions, therefore only weak bonds can be formed with linearly coordinated CO_2 molecules. Otherwise, the interaction of CO_2 molecule with surface basic sites implies a stronger bond, specifically, C and O atoms of CO_2 molecule can interact with surface O and adjacent cationic sites, respectively, therefore, in general, the formation of carbonate-like species produces high heats of interaction and formation of bonds hardly breakable. Considering the monolith case, SiO_2 oxide is enough apolar (due to the covalent bonds of the oxide framework) to avoid the interaction of silicon atoms with CO_2 molecules, but BBS, used as binder to produce monoliths, bring some inorganic components containing Ca^{2+} and Mg^{2+} cations responsible of the increase of the surface basicity. As a consequence, CO_2 can form stable carbonate-like species at the monolith surface, as demonstrated by the FTIR spectra carried out in the presence of CO_2 as probe molecule (see Figure 7).

FTIR spectroscopy allows revealing the vibrational features of samples, comprehensive of surface functional group vibrations. The spectra of plain FK and FK-NH_2 monoliths are quite different in terms of: i) intensity and shape of the broad signal in the range 3700-2500 cm^{-1} due to ν_{OH} interacting via H-bonding, ii) presence of a signal at 3200 cm^{-1} due to ν_{NH}, iii) intensity and shape of the large signal in the range 1800-1350 cm^{-1} due to ν_{OCO} of carbonate-like species. In all regions, FH-NH_2 sample shows the most intense signals, as the presence of polar amino groups favors the interaction of the surface with atmospheric water and CO_2 molecules. In addition NH_2 groups are responsible for the couple of bands at around 3200 cm^{-1}. The only signal not present in the FH-NH_2 spectrum is the narrow component at 3740 cm^{-1}, related to the presence of isolated non-interacting OH groups: this signal disappears after the grafting procedure which exploits the OH groups to bind the functionalizing molecules at the monolith surface. The interaction of the samples with CO_2 deserves a detailed description. As mentioned above, CO_2 molecules can interact linearly or in a bent form with an oxide surface: the two situations produce signals in the spectrum in the two regions evidenced in Figure 7: around 2340 cm^{-1} the linear form, in the range 1800-1350 cm^{-1} the bent forms. Looking at the spectra reported in Figure 7, it appears clearly that the linear interaction is mainly established on FK monolith, whereas both linear and bent interactions are present on FK-NH_2 sample, thanks to the presence of amino groups. In addition, the bent interactions are not completely reversible, as the bands formed by

CO_2 interaction in the low frequency range do not disappear completely during the vacuum outgassing of the sample at the temperature of the IR beam, indicating the probable formation of surface carbamate-like species. This results confirms the evidence obtained by the gas-volumetric adsorption measurements. The formation of carbamate-like species is a drawback of the material, as the regeneration of the adsorbing material at low temperature is not complete, nevertheless the amount of CO_2 reversibly bonded to the functionalized sample is enough high for justifying the deepening of this study.

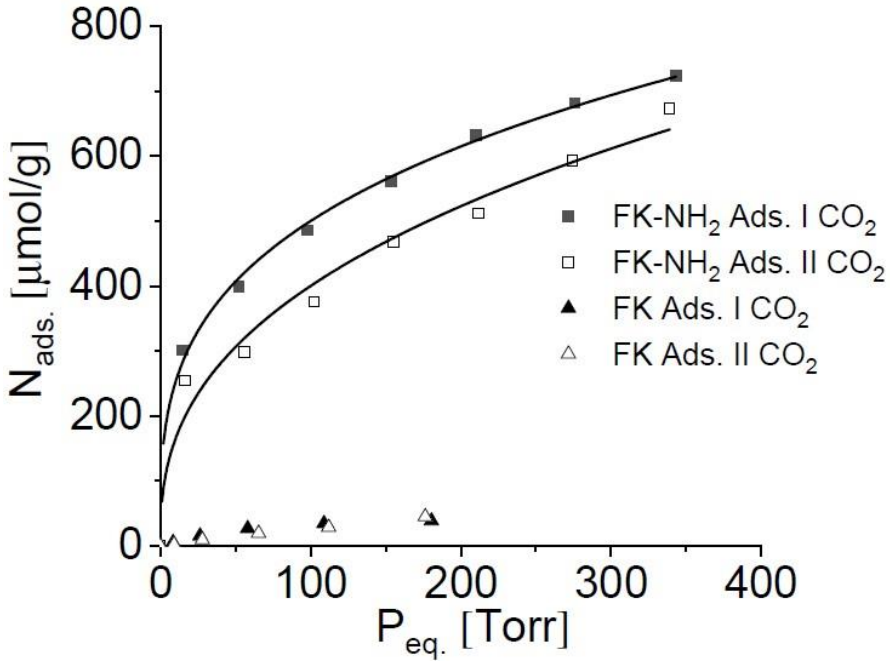

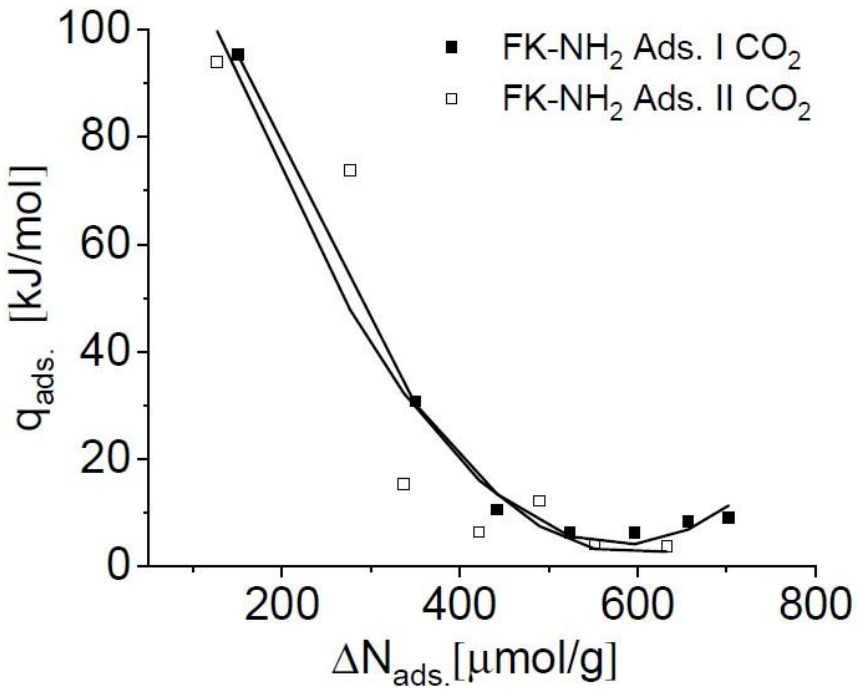

Figure 6: CO_2 adsorbed amounts (upper section) and adsorption heats (lower section) for FK monoliths. Full symbols: primary run, empty symbols: secondary run. The solid line curves represent a possible trend for an easy reading of the experimental points.

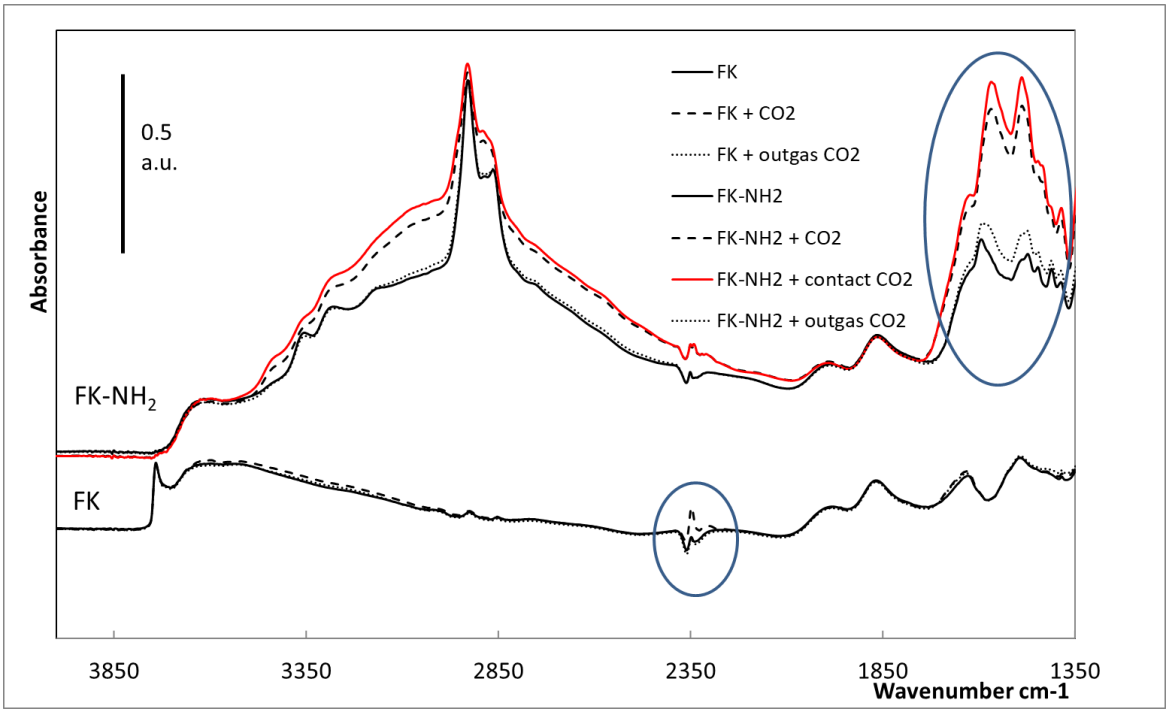

Figure 7: FTIR spectra of FK and FH-NH_2 monoliths activated at BT (IR Beam Temperature, solid line), after contact with 20 Torr CO_2 (broken line), after prolonged contact with CO_2 (red curve) and after CO_2 outgassing at BT (dotted line).

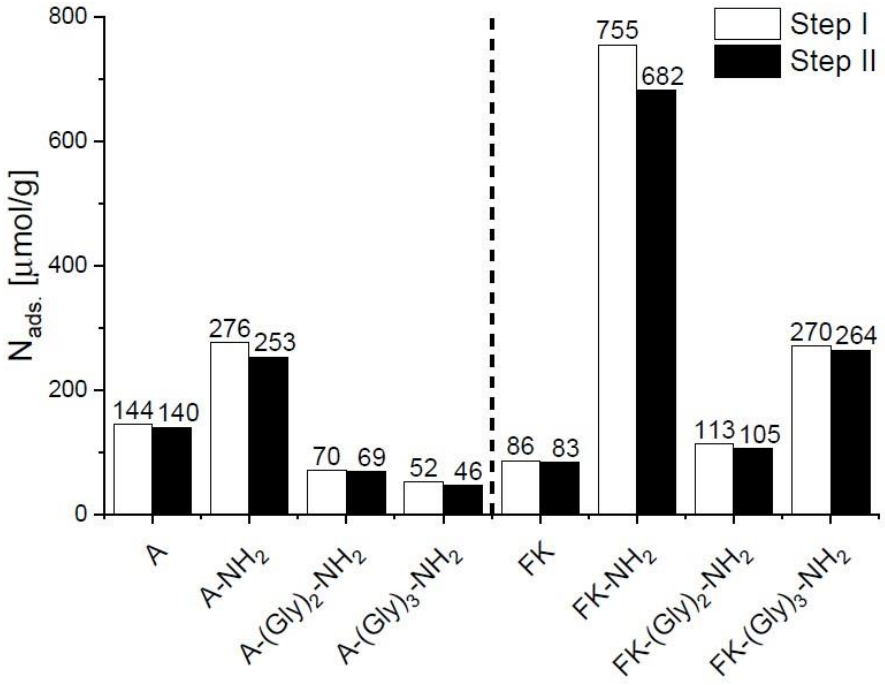

Figure 8: Summary of CO_2 adsorbed amounts obtained for the equilibrium pressure of 400 Torr, primary (Step I) and secondary (Step II) adsorption.

The summary of the main results obtained by gas-volumetric adsorption measurements are reported in Figure 8. The best samples for CO_2 capture are those functionalized with AMPS and the best one in absolute terms is FK-NH_2, leading to an amount of captured CO_2 of about 750 µmol/g for 400 Torr of equilibrium pressure.

The performance of this material was compared with that of a literature activated carbon [14] in order to establish a comparison with a known system and determine the applicability of monolith material in real applications. As visible in Figure 9, the comparison is encouraging and confirms a possible industrial application of FK-NH_2 material. In fact, the amount of CO_2 captured by activated carbon is only the double than that observed for the monolith material: it is expectable that an optimization of the adsorbent could increase that amount.

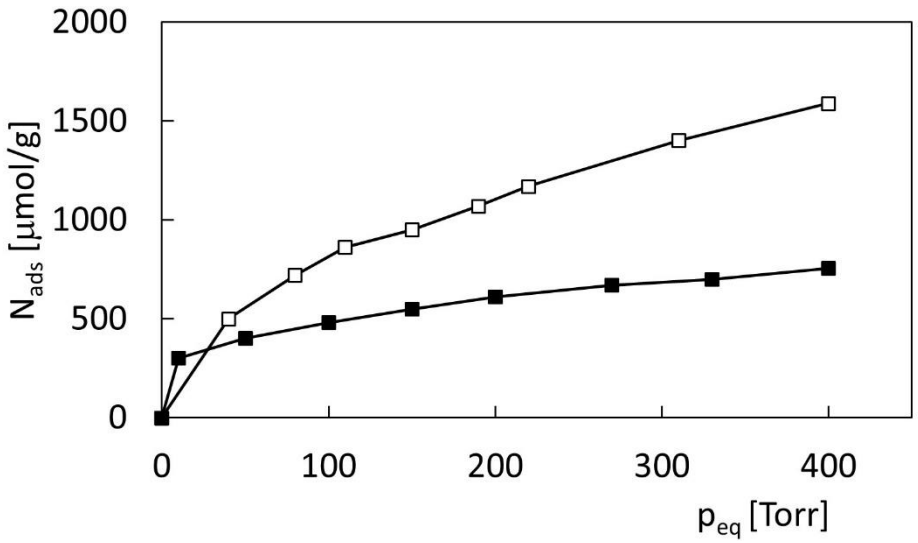

Figure 9: Comparison between adsorption capacity of an activated carbon from the literature [14] (white squares) and FK-NH_2 (black squares).

In order to optimize the efficiency obtained with FK-NH_2 sample, we tried to explain the possible reasons at the base of the good performance of this material. We can consider three main factors: the extension of the surface area, the efficiency of the functionalization (i.e., number of NH2 groups as calculated by Eq.2 and tabulated in Table 3, namely 6.5 10^{20} and 9.3 10^{20} NH_2 groups g^{-1} for A-NH_2 and FK-NH_2 respectively) and the hydrophilic/hydrophobic character of the support. For what concerns surface extension, A-NH_2 sample shows a higher SSA with respect to FK-NH_2, therefore this is not the crucial factor for the higher CO_2 adsorption observed. The functionalization extent for FK-NH_2 is 43% higher than that of A-NH_2, whereas the CO_2 adsorbed amount is about three times that measured for A-NH_2, so no direct correlation exists between the number of NH_2 groups available and the CO2 uptake. The only aspect explaining the trend of the results obtained is, therefore, the different polarity of the supports, that means that more polar surface attracts more efficiently CO_2 molecules. To test this hypothesis, water adsorption measurements were carried out on A and FK and the results are reported in Figure 10 in terms of adsorbed amount and heat of adsorption.

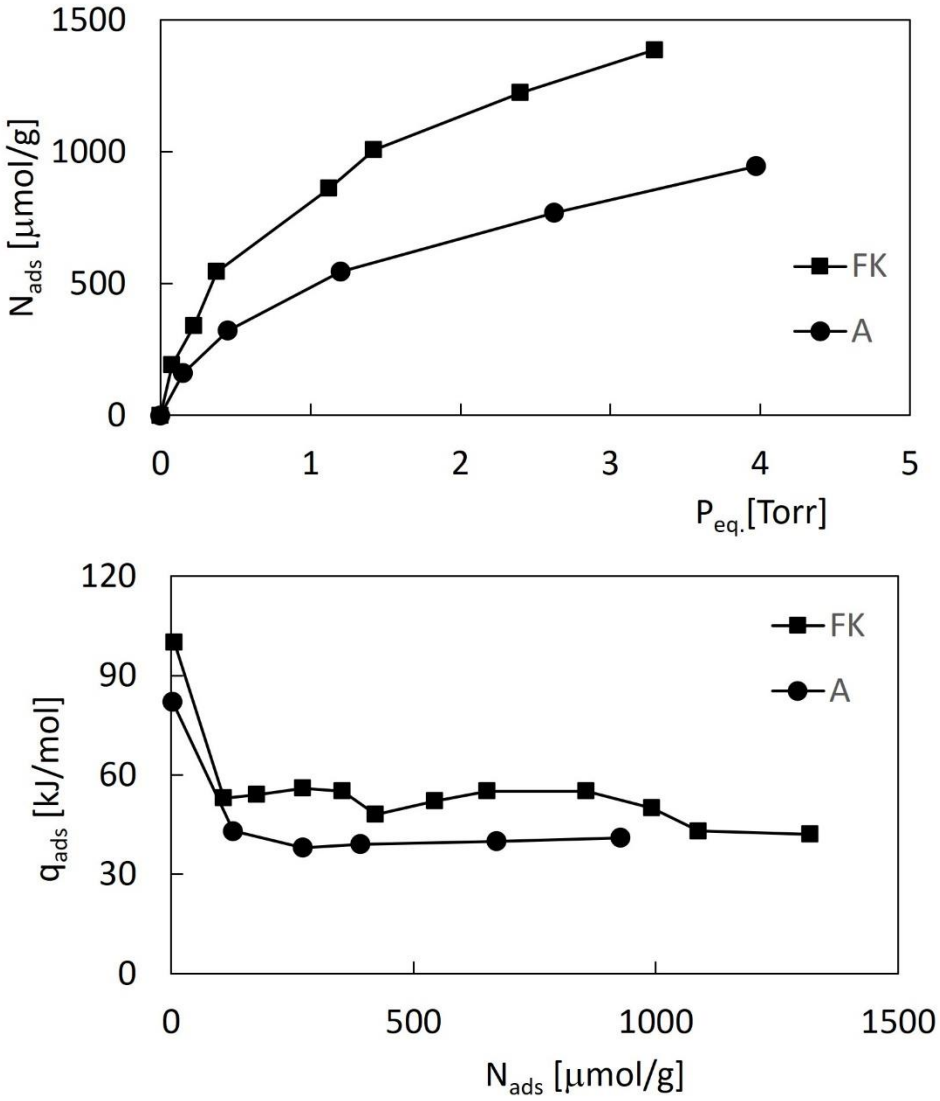

Figure 10: Gas-volumetric adsorption isotherms (upper section) and heats of adsorption (lower section) of water adsorbed at 30°C on A and FK monolith outgassed at 30°C.

As it can be seen, the FK monolith adsorbs a higher amount of water with higher heat of adsorption, indicating a higher polarity with respect to A monolith.

The other aspect to consider is the effect of the chain extension carried out with diGly and triGly which does not show great beneficial effects on CO_2 capture. Probably the inductive effects of amidic groups (2 groups in diGly sample and 3 groups in triGly sample) decrease the availability of amine N lone pair decreasing consequently the strength of the interaction with CO_2 molecules. As a proof of this hypothesis, samples experiencing a high yield of chain extension reaction (A-$(Gly)_2$-NH_2 and A-$(Gly)_3$-NH_2) possess limited amounts of residual propylamino-groups and consequently exhibit a limited ability in CO_2 capture. On the contrary, samples experiencing a low yield of chain

extension reaction (FK-$(Gly)_2$-NH_2 and FK-$(Gly)_3$-NH_2) possess higher amounts of residual propylamino-groups and consequently exhibit a higher efficiency in CO_2 capture.

4. Conclusions

The synthesis of hybrid organic-inorganic monoliths was successfully carried out with production of high surface area, mesoporous, handleable supports with good mechanical properties which can be efficiently surface-functionalized exploiting the reactivity of SiOH groups. Monoliths before and after surface modification were physico-chemically characterized in order to obtain insights about morphology, functionalization extension and thermal stability, and tested towards CO_2 capture at 30°C.

The propylamino-groups demonstrated to be the most efficient for support functionalization, as the presence of amidic groups, introduced during the chain extension reaction and bringing unfavorable inductive effects, produce less efficient materials, whose efficiency depends on the yield of the chain extension reaction.

The polarity of the support plays a fundamental role in the functionalization reaction, as the solvent used change the wettability of the monolith and consequently the reaction yield, but also the CO_2 capture process efficiency.

Last but not least, the monolith preparation method allows to reuse composted urban waste in a technological application that increases the importance and the economic value of the separated collection and recycle/reuse of organic residues extending the circular economy principles in the field of CO_2 capture.

5. Acknowledgments

Compagnia di San Paolo and University of Torino are gratefully acknowledged for funding (“Bando per il finanziamento ex-post di progetti di ricerca di Ateneo – anno 2018”).

6. References

[1] J.R. Fernández, S. Garcia, E.S. Sanz-Pérez, CO_2 Capture and Utilization Editorial, Ind. Eng. Chem. Res. 59(15) (2020) 6767–6772. https://doi.org/10.1021/acs.iecr.0c01643

[2] H. Wang, X. Li, Z. Cui, Z. Fu, L. Yang, G. Liu, M. Li, Coffee grounds derived N enriched microporous activated carbons: efficient adsorbent for post-combustion CO_2 capture and conversion, Journal of Colloid And Interface Science Volume 578

(2020) 491-499. https://doi.org/10.1016/j.jcis.2020.05.125

[3] C. Choi, R.L. Kadam, S. Gaikwad, K.S. Hwang, S. Han, Metal organic frameworks immobilized polyacrylonitrile fiber mats with polyethyleneimine impregnation for CO_2 capture, Microporous and Mesoporous Materials 296 (2020) 110006. https://doi.org/10.1016/j.micromeso.2020.110006

[4] J. Sreńscek-Nazzal, K. Kiełbasa, Advances in modification of commercial activated carbon for enhancement of CO_2 capture, Applied Surface Science, 494 (2019) 137–151. https://doi.org/10.1016/j.apsusc.2019.07.108

[5] D. Zabiegaj, M. Caccia, M.E. Casco, F. Ravera, J. Narciso, Synthesis of carbon monoliths with a tailored hierarchical pore structure for selective CO_2 capture. Journal of CO2 Utilization, 26 (2018) 36–44. https://doi.org/10.1016/j.jcou.2018.04.020

[6] C. Zhang, W. Song, G. Sun, L. Xie, J. Wang, K. Li, T. Drage, CO_2 capture with activated carbon grafted by nitrogenous functional groups. Energy and Fuels, 27(8) (2013) 4818–4823. https://doi.org/10.1021/ef400499k

[7] J.L. Shamshina, O. Zavgorodnya, R.D. Rogers, Ionic Liquids, in: Paul Worsfold, Colin Poole, Alan Townshend, Manuel Miró (Eds.), Encyclopedia of Analytical Science (Third Edition), Academic Press, Cambridge (Massachusetts), 2019, pp. 218-225. https://doi.org/10.1016/B978-0-12-409547-2.13931-9

[8] C.P. Cabello, G. Berlier, G. Magnacca, P. Rumori, G. Turnes Palomino, Enhanced CO_2 adsorption capacity of amine-functionalized MIL-100(Cr) metal-organic frameworks, CrystEngComm, 17(2) (2015) 430–437. https://doi.org/10.1039/c4ce01265h

[9] A. Anceschi, G. Magnacca, F. Trotta, M. Zanetti, Preparation and characterization of microporous carbon spheres from high amylose pea maltodextrin, RSC Advances, 7(57) (2017) 36117–36123. https://doi.org/10.1039/c7ra05343f

[10] N. Politakos, I. Barbarin, L.S. Cantador, J.A. Cecilia, E. Mehravar, R. Tomovska, Graphene-Based Monolithic Nanostructures for CO_2 Capture, Industrial & Engineering Chemistry Research, 59(18) (2020) 8612–8621. https://doi.org/10.1021/acs.iecr.9b06998

[11] V. Jiménez, A. Ramírez-Lucas, J.A., Díaz, P. Sánchez, A. Romero, CO_2 capture in different carbon materials. Environmental Science and Technology, 46(13) (2012) 7407–7414. https://doi.org/10.1021/es2046553

[12] C. Lu, H. Bai, B. Wu, F. Su, J.F. Hwang, Comparative study of CO_2 capture by carbon nanotubes, activated carbons, and zeolites, Energy and Fuels, 22(5) (2008) 3050–3056. https://doi.org/10.1021/ef8000086

[13] S. García, J.J. Pis, F. Rubiera, C. Pevida, Predicting Mixed-Gas Adsorption Equilibria on Activated Carbon for Precombustion CO_2 Capture Langmuir 29(20) (2013) 6042–6052. https://doi.org/10.1021/la4004998

[14] M.G. Plaza, I. Durán, N. Querejeta, F. Rubiera, C. Pevida, Experimental and

Simulation Study of Adsorption in Postcombustion Conditions Using a Microporous Biochar. 2. H_2O, CO_2, and N_2 Adsorption, Industrial and Engineering Chemistry Research 55(24) (2016) 6854–65. https://doi.org/10.1021/acs.iecr.6b01720

[15] M. Karimi, J.A.C. Silva, C. N. D. P. Gonçalves, J. L. Diaz De Tuesta, A.E. Rodrigues, H.T. Gomes, CO_2 Capture in Chemically and Thermally Modified Activated Carbons Using Breakthrough Measurements: Experimental and Modeling Study, Industrial and Engineering Chemistry Research, 57(32) (2018) 11154–11166. https://doi.org/10.1021/acs.iecr.8b00953

[16] W. Dong, X. Chen, Y. Wu, TiO_2-Doped K_2CO_3/Al_2O_3 Sorbents for CO_2 Capture, Energy and Fuels, 52(10) (2016) 1073–1080. https://doi.org/10.1021/ef500133e

[17] S. Gao, D. Guo, H. Jin, S. Li, J. Wang, S. Wang, Potassium Carbonate Slurry-Based CO_2 Capture Technology, Energy and Fuels, 29(10) (2015) 6656–6663. https://doi.org/10.1021/acs.energyfuels.5b01421

[18] J.J. Lee, C. Sievers, C.W. Jones, Silica-Supported Hindered Aminopolymers for CO_2 Capture, Industrial and Engineering Chemistry Research, 58(50) (2019) 22551–22560. https://doi.org/10.1021/acs.iecr.9b02220

[19] L. Li, X. Wen, X. Fu, F. Wang, N. Zhao, F. Xiao, W. Wie, Y. Sun, MgO/Al_2O_3 sorbent for CO_2 capture, Energy and Fuels, 24(10) (2010) 5773–5780. https://doi.org/10.1021/ef100817f

[20] Y. Sun, J. Zhao, J. Wang, N. Tang, R. Zhao, D. Zhang, K. Li, Sulfur-Doped Millimeter-Sized Microporous Activated Carbon Spheres Derived from Sulfonated Poly(styrene-divinylbenzene) for CO_2 Capture, Journal of Physical Chemistry C, 121(18) (2017) 10000–10009. https://doi.org/10.1021/acs.jpcc.7b02195

[21] C. Xu, N. Hedin, Microporous adsorbents for CO_2 capture - A case for microporous polymers?, Materials Today, 17(8) (2014) 397–403. https://doi.org/10.1016/j.mattod.2014.05.007

[22] P. Teixeira, J. Hipólito, A. Fernandes, F. Ribeiro, C.I.C. Pinheiro, Tailoring Synthetic Sol-Gel CaO Sorbents with High Reactivity or High Stability for Ca-Looping CO_2 Capture, Industrial and Engineering Chemistry Research, 58(19) (2019) 8484–8494. https://doi.org/10.1021/acs.iecr.8b05311

[23] C. Hou, N. Ghéczy, D. Messmer, K. Szymańska, J. Adamcik, R. Mezzenga, A.B. Jarzebski, P. Walde, Stable Immobilization of Enzymes in a Macro- and Mesoporous Silica Monolith, ACS Omega, 4(4) (2019) 7795–7806. https://doi.org/10.1021/acsomega.9b00286

[24] J. Kecht, T. Bein, Functionalization of colloidal mesoporous silica by metalorganic reagents, Langmuir, 24(24) (2008) 14209–14214. https://doi.org/10.1021/la802115n

[25] N.P. Sajo, W. Fan, T. Yokoi, T. Okubo, Synthesis of a Three-Dimensional Cubic

Mesoporous Silica Monolith Employing an Organic Additive through an Evaporation-Induced Self-Assembly Process, Langmuir 22(14) (2006) 6391–97.

[26] W. Yantasee, R.D. Rutledge, W. Chouyyok, V. Sukwarotwat, G. Orr, C.L. Warner, M.G. Warner, G.E. Fryxell, R.J. Wiacek, C. Timchalk, R.S. Addleman, Functionalized Nanoporous Silica for the Removal of Heavy Metals from Biological Systems: Adsorption and Application, ACS Applied Materials and Interfaces, 2(10) (2010) 2749–58. https://doi.org/10.1021/am100616b

[27] E. Soto-Cantu, R. Cueto, J. Koch, P.S. Russo, Synthesis and Rapid Characterization of Amine-Functionalized Silica, Langmuir 28(13) (2012) 5562–69. https://doi.org/10.1021/la204981b

[28] G. Osei-Prempeh, H.J. Lehmler, S.E. Rankin, B.L. Knutson, Direct Synthesis and Accessibility of Amine-Functionalized Mesoporous Silica Templated Using Fluorinated Surfactants, Industrial and Engineering Chemistry Research 50(9) (2011) 5510–22. https://doi.org/10.1021/ie101313t

[29] Ko Young Gun, Hyun Jeong Lee, Jae Yong Kim and Ung Su Choi, Hierarchically Porous Aminosilica Monolith as a CO_2 Adsorbent, ACS Applied Materials and Interfaces 6(15) (2014) 12988–96. https://doi.org/10.1021/am5029022

[30] S. Builes, V.F. Lourdes, Understanding CO_2 Capture in Amine-Functionalized MCM-41 by Molecular Simulation, Journal of Physical Chemistry C 116(4) (2012) 3017–24. https://doi.org/10.1021/jp210494f

[31] F.S. Taheri, A. Ghaemi, A. Maleki, S. Shahhosseini, High CO_2 Adsorption on Amine-Functionalized Improved Mesoporous Silica Nanotube as an Eco-Friendly Nanocomposite, Energy and Fuels 33(6) (2019) 5384–97. https://doi.org/10.1021/acs.energyfuels.9b00703

[32] K. Gdula, A. Gładysz-Płaska, B. Cristóvão, W. Ferenc, E. Skwarek, Amine-Functionalized Magnetite-Silica Nanoparticles as Effective Adsorbent for Removal of Uranium(VI) Ions, Journal of Molecular Liquids 290(11) (2019) 12–17. https://doi.org/10.1016/j.molliq.2019.111217

[33] H.-T. Fan, X. Fan, J. Li, M. Guo, D. Zhang, F. Yan, T. Sun, Selective Removal of Arsenic(V) from Aqueous Solution Using a Surface-Ion-Imprinted Amine-Functionalized Silica Gel Sorbent, Industrial and Engineering Chemistry Research 51(14) (2012) 5216–23. https://doi.org/10.1021/ie202655x

[34] N. Saravanan, Y. Jeon, S.S. Park, C.-S. Ha, Hexadecyltrimethylammonium Bromide Surfactant-Supported Silica Material for the Effective Adsorption of Metanil Yellow Dye, ACS Omega 4(5) (2019) 8548–58. https://doi.org/10.1021/acsomega.9b00533

[35] T. Cai, H. Zhang, J. Chen, Z. Li, H. Qiu, Polyethyleneimine-Functionalized Carbon Dots and Their Precursor Co-Immobilized on Silica for Hydrophilic Interaction Chromatography, Journal of Chromatography A 1597(6) (2019) 142–48. https://doi.org/10.1016/j.chroma.2019.03.026

[36] J.C.S. Terra, A. Moores, F.C.C. Moura, Amine-Functionalized Mesoporous Silica as a Support for on-Demand Release of Copper in the A3 -Coupling Reaction: Ultralow Concentration Catalysis and Confinement Effect, ACS Sustainable Chemistry and Engineering 7(9) (2019) 8696–8705. https://doi.org/10.1016/j.chroma.2019.03.026

[37] L.F. De Oliveira, K. Bouchmella, K. De Almeida Gonçalves, J. Bettini, J. Kobarg, M. Borba Cardoso, Functionalized Silica Nanoparticles as an Alternative Platform for Targeted Drug-Delivery of Water Insoluble Drugs, Langmuir 32(13) (2016) 3217–25. https://doi.org/10.1021/acs.langmuir.6b00214

[38] K.L. Reddy, K.S. Peeyush, S. Ashutosh, K. Ajay, R.S. Konathala, S. Yashveer, G. Neha, K. Venkata, Amine-Functionalized, Porous Silica-Coated NaYF 4 :Yb/Er Upconversion Nanophosphors for Efficient Delivery of Doxorubicin and Curcumin, Materials Science and Engineering C 96 (2019) 86–95. https://doi.org/10.1016/j.msec.2018.11.007

[39] N. Moitra, I. Shun, K. Toshiyuki, K. Kazuyoshi, Z. Yang, T. Kazuyuki, N. Kazuki, S. Toyoshi, Surface Functionalization of Silica by Si-H Activation of Hydrosilanes, Journal of the American Chemical Society 136(33) (2014) 11570–73. https://doi.org/10.1021/ja504115d

[40] V. Morales, M.N. Idso, M. Balabasquer, B. Chmelka, R.A. García-Muñoz, Correlating Surface-Functionalization of Mesoporous Silica with Adsorption and Release of Pharmaceutical Guest Species, Journal of Physical Chemistry C 120(30) (2016) 16887–98. https://doi.org/10.1021/acs.jpcc.6b06238

[41] G. Magnacca, F. Neves Dos Santos, R. Sadraei, Bio-based substances from compost as reactant and active phase for selective capture of cationic pollutants from waste water, Frontiers in Chemistry – Green and Sustainable Chemistry, special issue “Chemistry, a Sustainable Bridge from Waste to Materials for Energy and Environment”, 8 (2020) 550. https://doi.org/10.3389/fchem.2020.00550

[42] R. Sadraei, R.S. Murphy, E. Laurenti, G. Magnacca, Characterization Methodology to Evaluate the Activity of Supported Soybean Peroxidase, Materials and Interfaces 58(41) (2019) 19082-19089. https://doi.org/10.1021/acs.iecr.9b03495

[43] R. Sadraei, M.C. Paganini, P. Calza, G. Magnacca, An Easy Synthesis for Preparing Bio-Based Hybrid Adsorbent Useful for Fast Adsorption of Polar Pollutants, Nanomaterials 9(5) (2019) 731. https://doi.org/10.3390/nano9050731

[44] Q. Hu, J.E. Hampsey, N. Jiang, C. Li, Y. Lu, Surfactant-Templated Organic Functionalized Mesoporous Silica with Phosphino Ligands, Chemistry of Materials 17(6) (2005) 1561–69. https://doi.org/10.1021/cm0491983

[45] X. Du, J. He, Hierarchically Mesoporous Silica Nanoparticles: Extraction, Amino-Functionalization, and Their Multipurpose Potentials, Langmuir 27(6) (2011) 2972–79. https://doi.org/10.1021/la200014w

[46] Y.-S. Jun, Y.S. Huh, H.S. Park, A. Thomas, S.J. Jeon, E.Z. Lee, H.J. Won, W.H. Hong, S.Y. Lee, Y.K. Hong, Adsorption of Pyruvic and Succinic Acid by Amine-

Functionalized SBA-15 for the Purification of Succinic Acid from Fermentation Broth, Journal of Physical Chemistry C 111(35) (2007) 13076–86. https://doi.org/10.1021/jp072606g

[47] M. Etienne, S. Goubert-Renaudin, Y. Rousselin, C. Marichal, F. Denat, B. Lebeau, A. Walcarius, Multiarm Cyclam-Grafted Mesoporous Silica: A Strategy to Improve the Chemical Stability of Silica Materials Functionalized with Amine Ligands, Langmuir 25(5) (2009) 3137–45. https://doi.org/10.1021/la8032379

[48] R. Campos, A.J. Guenthner, T.S. Haddad, J.M. Mabry, Fluoroalkyl-Functionalized Silica Particles: Synthesis, Characterization, and Wetting Characteristics, Langmuir 27(16) (2011) 10206–15. https://doi.org/10.1021/la201545a

[49] M.L. Testa, M.L. Tummino, S. Agostini, P. Avetta, F. Deganello, E. Montoneri, G. Magnacca, A. Bianco Prevot, Synthesis, Characterization and Environmental Application of Silica Grafted Photoactive Substances Isolated from Urban Biowaste, RSC Advances 5(59) (2015) 47920–27. https://doi.org/10.1039/C5RA03164H

[50] M.L. Tummino, M.L. Testa, M. Malandrino, R. Gamberini, A. Bianco Prevot, G. Magnacca, E. Laurenti, Green waste-derived substances immobilized on SBA-15 silica: surface properties, adsorbing and photosensitizing activities towards organic and inorganic substrates, Nanomaterials, 9(2) (2019) 162-175. https://doi.org/10.3390/nano9020162

[51] M.L. Testa, V. La Parola, A.M. Venezia, Transesterification of Short Chain Esters Using Sulfonic Acid-Functionalized Hybrid Silicas: Effect of Silica Morphology, Catalysis Today 223 (2014) 115–21. https://doi.org/10.1016/j.cattod.2013.09.029

[52] Z. Bahrami, A. Badiei, F. Atyabi, Surface Functionalization of SBA-15 Nanorods for Anticancer Drug Delivery, Chemical Engineering Research and Design 92(7) (2014) 1296–1303. https://doi.org/10.1016/j.cherd.2013.11.007

[53] F. Feil, V. Cauda, T. Bein, C. Bräuchle, Direct Visualization of Dye and Oligonucleotide Diffusion in Silica Filaments with Collinear Mesopores, Nano Letters 12(3) (2012) 1354–61. https://doi.org/10.1021/nl2039474

[54] J.L. Steinbacher, C.C. Landry, Adsorption and Release of SiRNA from Porous Silica, Langmuir 30(15) (2014) 4396–4405. https://doi.org/10.1021/la402850m

[55] J. Ma, L. Zhen, Q. Xiaoqiang, D. Qiliang, T. Dingyin, Z. Lihua, Z. Yukui, Organic-Inorganic Hybrid Silica Monolith Based Immobilized Trypsin Reactor with High Enzymatic Activity, Analytical Chemistry 80(8) (2008) 2949–56. https://doi.org/10.1021/ac702343a

[56] R. El-Debs, F. Cadoux, L. Bois, A. Bonhommé, J. Randon, D. Vincent, C. Demesmay, Synthesis and Surface Reactivity of Vinylized Macroporous Silica Monoliths: One-Pot Hybrid versus Postsynthesis Grafting Strategies, Langmuir 31(42) (2015) 11649–58. https://doi.org/10.1021/acs.langmuir.5b02681

[57] C.H. Pélisson, N. Takahiro, Z. Yang, M. Kei, K. Toshiyuki, M. Ayaka, K. Hironori, M. Shunki, T. Masamoto, K. Kazuyoshi, S. Toyoshi, N. Kazuki, Grafted Polymethylhydrosiloxane on Hierarchically Porous Silica Monoliths: A New Path to Monolith-Supported Palladium Nanoparticles for Continuous Flow Catalysis Applications, ACS Applied Materials and Interfaces 9(1) (2017) 406–12. https://doi.org/10.1021/acsami.6b12653

[58] C. Hou, J. Ma, D. Tao, Y. Shan, Z. Liang, L. Zhang, Y. Zhang, Organic-Inorganic Hybrid Silica Monolith Based Immobilized Titanium Ion Affinity Chromatography Column for Analysis of Mitochondrial Phosphoproteome, Journal of Proteome Research 9(8) (2010) 4093–4101. https://doi.org/10.1021/pr100294z

[59] G. Magnacca, E. Laurenti, E. Vigna, F. Franzoso, L. Tomasso, E. Montoneri, V. Boffa, Refuse Derived Bio-Organics and Immobilized Soybean Peroxidase for Green Chemical Technology, Process Biochemistry 47(12) (2012) 2025–31. https://doi.org/10.1016/j.procbio.2012.07.021

[60] V. Boffa, L. Parmeggiani, N.A. Haaning, G. Magnacca, Hydrophilicity and Surface Heterogeneity of TiO2-Doped Silica Materials for Membrane Applications, Microporous and Mesoporous Materials 221 (2016) 81–90. https://doi.org/10.1016/j.micromeso.2015.09.017

[61] A. Cauvel, D. Brunel, F. Di Renzo, E. Garrone, B. Fubini, Hydrophobic and Hydrophilic Behavior of Micelle-Templated Mesoporous Silica, Langmuir 13(10) (1997) 2773–78. https://doi.org/10.1021/la962059i